Bonding characteristics in NiAl intermetallics with O impurity: a first-principles computational tensile test

2009 J. Phys.: Condens. Matter 21 025402

(http://iopscience.iop.org/0953-8984/21/2/025402)

IOP PUBLISHING JOURNAL OF PHYSICS: CONDENSED MATTER

J. Phys.: Condens. Matter **21** (2009) 025402 (6pp) doi:10.1088/0953-8984/21/2/025402

Bonding characteristics in NiAl intermetallics with O impurity: a first-principles computational tensile test

Xue-Lan Hu, Ying Zhang, Guang-Hong Lu[1] and Tianmin Wang

Department of Physics, Beijing University of Aeronautics and Astronautics, Beijing 100191, People's Republic of China

E-mail: LGH@buaa.edu.cn

Received 12 September 2008, in final form 28 October 2008
Published 10 December 2008
Online at stacks.iop.org/JPhysCM/21/025402

Abstract

We have performed a first-principles computational tensile test on NiAl intermetallics with O impurity along the [001] crystalline direction on the (110) plane to investigate the tensile strength and the bonding characteristics of the NiAl–O system. We show that the ideal tensile strength is largely reduced due to the presence of O impurity in comparison with pure NiAl. The investigations of the atomic configuration and bond-length evolution show that O prefers to bond with Al, forming an O–Al cluster finally with the break of O–Ni bonds. The O–Ni bonds are demonstrated to be weaker than the O–Al bonds, and the reduced tensile strength originates from such weaker O–Ni bonds. A void-like structure forms after the break of the O–Ni and some Ni–Al bonds. Such a void-like structure can act as the initial nucleation or the propagation path of the crack, and thus produce large effects on the mechanical properties of NiAl.

(Some figures in this article are in colour only in the electronic version)

1. Introduction

The ideal strength of a crystal is determined by the maximum stress at elastic instability (yield or break) when applying an increasing stress to an infinite, perfect (defect-free) crystal [1, 2]. It forms an upper limit to the strength of a real crystal, which is of both scientific and engineering interest [2, 3]. The ideal strength is an intrinsic material property that is determined by the behavior of valence electrons and ions. Similarly, the ideal strength of an ideal defective system containing point defects, grain boundaries or impurity atoms can be determined as the maximum stress required to reach elastic instability under increasing load without introducing extrinsic dislocation or cracks. This can be regarded as intrinsic local strength of a defect region in real materials. It is of great importance to investigate the ideal strength of both perfect and defective systems in order to understand the mechanical properties of materials.

By virtue of the development of the density-functional theory (DFT) [4, 5] combined with the band-theoretical schemes and the rapid progress of modern computers, it became possible to perform a first-principles computational tensile test (FPCTT) to investigate the stress as a function of strain and obtain the ideal tensile strengths by deforming crystals to failure [3]. In FPCTT, symmetry is generally an important factor to determine the stress–strain relation and the calculated ideal strength. Many studies focus on the ideal strength of single crystals such as W [6, 7], Cu [8], Mo [9], Nb [9], Al [8, 10], Ni [11], Fe [12] and some ordered compound such as β-SiC [13] and SiN [14, 15] have been reported. The FPCTT has also been employed in pure intermetallic compound systems such as Ni(Fe, Co)Al [16] and Al_3 (V, Ti) [17]. On the other hand, the ideal strength can also be extended to the systems containing defects such as a point defect [18], an interface [19, 20] or a grain boundary [21–26].

NiAl intermetallics exhibit many interesting properties including high strength, high melting temperature and high corrosion resistance, and thus can be employed in the aerospace industry as a high-temperature structural material [27, 28]. However, poor ductility at low temperatures and low strength at elevated temperature limits its technological assignments and applications [27, 28]. Many

[1] Author to whom any correspondence should be addressed.

attempts have been made in order to improve the room temperature ductility of NiAl by investigating effects of microalloying, macroalloying and reinforcing the ductile second phase [29–35]. Despite these attempts, the room temperature brittleness is still a key problem for NiAl applications as a high-temperature material.

It is generally accepted that a trace amount (ppm) of an impurity can result in a large mechanical property variation of materials [21–26]. Impurity is one of the uncontrollable factors that can have strong effects on the mechanical properties of NiAl [36]. There are several kinds of impurities including O, B, C, N, Si, P and S in NiAl [27]. We have performed first-principles calculations to investigate the atomic and electronic structures of NiAl with O impurity in previous work [37] and found that O tends to form an Al_2O_3-like tetrahedron structure with its nearest Al or Ni atoms, leading to the formation of the stronger O–Al bond containing a covalent component. This can cause an increase of the brittleness and a decrease of the ductility of NiAl based on the calculated elastic constants and the empirical criteria.

In this paper, we calculate the ideal tensile strength of NiAl with O impurity by using FPCTT and describe the behavior of NiAl with O through the observed bond-length and atomic configuration evolution in the tensile process. The results contribute to the further understanding of the effect of O impurity on the mechanical properties of NiAl.

2. Computational details

We employ a first-principles method based on DFT using VASP [38]. The ion–electron interaction is described by the ultrasoft pseudopotential [39], and the exchange–correlation function is described within the generalized gradient approximation according to the parameterization of Perdew and Wang [40]. The plane-wave cutoff energy is 25 Ryd. The supercell of NiAl with cubic B2 structure is constructed containing 54 atoms with one O impurity atom in one of the tetrahedral interstitial sites in the supercell. The supercell is sampled by the $(4 \times 5 \times 5)$ $\boldsymbol{k}$-point grids according to the Monkhorst–Pack scheme [41] according to the optimized lattice parameters of 8.72 Å × 8.26 Å × 8.26 Å in all the three crystalline directions of [001], [110] and [$\bar{1}$10]. The calculated equilibrium lattice parameter is 2.891 Å for the B2-NiAl, in good agreement with the corresponding experimental value of 2.89 Å. The energy relaxation is continued until the force on all the atoms is converged to less than 10^{-3} eV Å^{-1}.

The experimental results indicate that the major deformation mode of B2-NiAl is the ⟨001⟩ {110} slip [27]. We thus choose the [001] direction on the (110) plane as the tensile direction. For the uniaxial tensile strain, the tensile stress σ is calculated from

$$\sigma = \frac{1}{\Omega(\varepsilon)} \frac{\partial E}{\partial \varepsilon}, \tag{1}$$

where E is the total energy and $\Omega(\varepsilon)$ is the volume at a given tensile strain of ε.

In the tensile test, a uniaxial tensile strain is introduced and the supercell is stretched by a small increment in the [001] direction. The strain is determined by

$$\varepsilon = (l_\varepsilon - l_0)/l_0, \tag{2}$$

where l_ε is the length of the cell in the [001] direction with the strain ε and l_0 is that of the initial cell. Poisson's effect is considered in the FPCTT by fully relaxing the cell lengths in the [110] and [$\bar{1}$10] directions until the stresses in these two directions are less than 0.1 GPa.

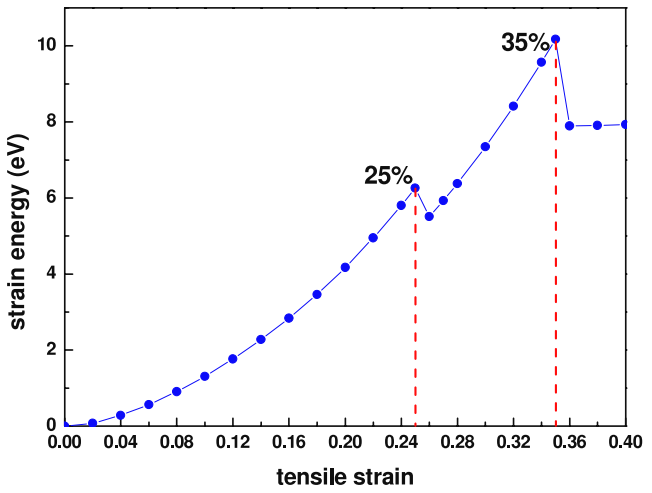

Figure 1. Strain energy of the NiAl–O system as a function of tensile strain by FPCTT. The zero reference energy is set as the energy at zero strain.

3. Results and discussion

3.1. Theoretical tensile strength

The strain energy as a function of tensile strain for the NiAl–O system is shown in figure 1. Strain energy increases with increasing tensile strain until the strain of 25%, at which the strain energy decreases and then increases again. The strain energy shows a sharp drop at a strain of 35% after a continuous increase with increasing strain and remains almost unchanged afterward, which implies that the system becomes stable beyond the strain 35%.

Stress evolution with increasing strain for the NiAl–O system in the [001] direction is straightforwardly shown in figure 2. The strain increase leads to a continuous stress increase until a strain of 25%, with the appearance of first maximum stress of 15.2 GPa corresponding to the first energy maximum in the energy–strain curve (figure 1). Beyond the strain of 25%, the stress starts to decrease and reaches a minimum of 13.3 GPa at a strain of 26%, of which the energy decreases correspondingly (figure 1). Despite such a stress decrease, fracture has not occurred yet because the energy increases continuously (figure 1). Afterward, the stress increases again to the second stress maximum of 21.1 GPa at the strain of 35% corresponding to the second energy maximum (figure 1), and drops suddenly to 0.72 GPa. The fracture should occur here, but needs further investigation. So, the ideal tensile strength of the NiAl–O system is 21.1 GPa.

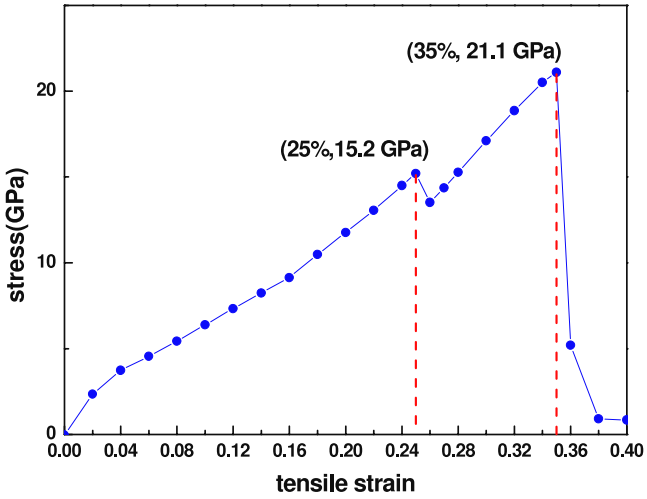

Figure 2. Stress in the [001] direction of the NiAl–O system as a function of strain by FPCTT.

In comparison with pure NiAl, the tensile strength of which is 37.6 GPa according to the present calculation, the tensile strength is reduced due to the presence of the O impurity.

It should be noted that the tensile strength here is a gauge-dependent quantity, which depends on the supercell size, similar to the calculated average stress for a certain specialized supercell [42]. As a matter of fact, the tensile strength of the NiAl–O system will increase with increasing supercell size, and will finally converge to the strength of pure NiAl. However, such 'local' tensile strength reduction still reflects the local variation of the mechanical property. In the following, we will further see the local bonding characteristic in the tensile process due to the introduction of O.

3.2. Atomic configuration and bond length

In order to understand the effect of the O impurity on the ideal tensile strength of NiAl from an atomic view, we investigate atomic configuration and bond-length evolution with increasing strain for the NiAl–O system. We choose the representative strains of 0%, 25%, 26%, 35%, 36% and 40% in the tensile process, which corresponds to the initial zero strain, and the strain before and after the first and second stress maximum, respectively, as shown in figure 3. The letters *A*, *B* and *O* represent the Al, Ni and O atoms, respectively. We choose the bonds between O and its first-nearest-neighbor (1NN) Ni (*B1*, *B2*) and Al (*A1*, *A2* at the beginning of the tensile process and *A1*, *A3* after the strain 26%) atoms (figure 4(a)) as well as some Ni–Al bonds (figure 4(b)). We choose six representative Ni–Al bonds, i.e. *A1B3*, *A2B2*, *A3B2*, *A3B6*, *A5B5* and *A6B3*.

The most energetically favorable site of O in NiAl is the tetrahedral interstitial site [37]. So, at the initial zero strain state, the bond length of O–Al is 1.77 Å (*OA1*, *OA2*) while the bond length of O–Ni (*OB1*, *OB2*) is 1.99 Å. Both are exactly the same as in our previous study [37]. *A3* is 2NN of O at zero strain, and the distance between *A3* and O is 2.78 Å. Due to the presence of O atoms, the Ni–Al bonds *A2B2*, *A3B2* close to the O atom are much longer than those Ni–Al bonds in pure NiAl (2.50 Å). Further, the bond length of *A2B2* (2.91 Å) is larger than the bond length of *A3B2* (2.64 Å). It is because *A2* is the 1NN of the O atom while *A3* is the 2NN of the O atom at the strain zero. This implies that the presence of O can weaken the surrounding Ni–Al bonds, as reflected in the tensile process.

It is clearly shown in figure 4 that *OA1*, *OA2* and most of the Ni–Al bonds extend with the strain increase until the strain of 25%. After this strain, *OA2* increases rapidly from 1.92 Å (at strain 25%) to 3.14 Å (at the strain 26%), while *OA3* decreases from 2.83 to 1.78 Å with the same bond length as *OA1* at the strain 26%. This indicates the *OA2* bond break. Both *OB1* and *OB2* have a negligible change with bond length of 1.97 Å. This is because the angles between *OA1* (*OA2*) and the [001] tensile direction are 26.5°, while *OB1* and *OB2* are perpendicular to the tensile direction, as shown in figure 5(a). Such configuration characteristic with respect to the tensile direction gives rise to the break of one of the O–Al bonds, making the O atom bond with another Al atom *A3*. Such structure transformation during the tensile process is clearly shown in figures 3(b) and (c) corresponding to the strain 25% and 26%, respectively. Consequently, the Ni–Al bond *A2B2* contracts from 2.90 Å at the strain 25% to 2.63 Å at the strain 26%, while *A3B2* extends from 2.86 to 3.12 Å. Therefore, the first stress maximum originates from the break of the O–Al bond *OA2*.

As illustrated above, the 1NNs of O changes from *A1*, *A2*, *B1* and *B2* to *A1*, *A3*, *B1* and *B2* at the strain 26%. At this strain, the angles of both the O–Al bonds (*OA1*, *OA3*) and the O–Ni bonds (*OB1*, *OB2*) with respect to the tensile direction is 52.5°, as shown in figure 5(b), quite different from those angles before 26% (figure 5(a)). Also, in figures 3, *A2*, *A4*, *B3* and *B4* are the 2NNs of O, and *A5*, *A6*, *B5* and *B6* are the 3NN.

After the first stress maximum, the obvious phenomenon is that the O–Ni bonds of *OB1* and *OB2* extend rapidly starting from the strain 35%. Some Ni–Al bonds including *A3B2*, *A3B6*, *A5B5* and *A6B3* exhibit similar behavior at this strain. These indicate the break of the O–Ni bonds and those Ni–Al bonds, which contribute to the second stress maximum. The bond length of *OB1* and *OB2* increases to 3.06 and 2.18 Å at the strain 36%. The Ni–Al bonds *A1B3*, *A3B2*, *A3B6*, *A5B5* and *A6B3* extend to 3.67 Å, 3.95 Å, 4.18 Å, 3.72 Å and 3.63 Å at the strain 36%, respectively. This suggests the O–Ni bonds are weaker as compared with O–Al, leading to the break of these O–Ni bonds in the tensile process. The extended Ni–Al bonds (due to the presence of O) close to these weaker O–Ni bonds also break. The break of both O–Ni and Ni–Al bonds results in the formation of a void-like structure, as shown in figures 3(e) and (f). Such a void-like structure expands with further strain increase. The void-like structure can act as the initial nucleation or the propagation path of crack, and thus have a significant effect on the mechanical properties of the NiAl.

O finally bonds merely with the Al atoms of *A1*, *A3* and *A5* after the formation of the void-like structure, forming an O–Al cluster. This obviously suggests that O prefers to bond with Al instead of Ni, and the O–Al bond is stronger than O–Ni, consistent with the previous study [37]. The reduced tensile

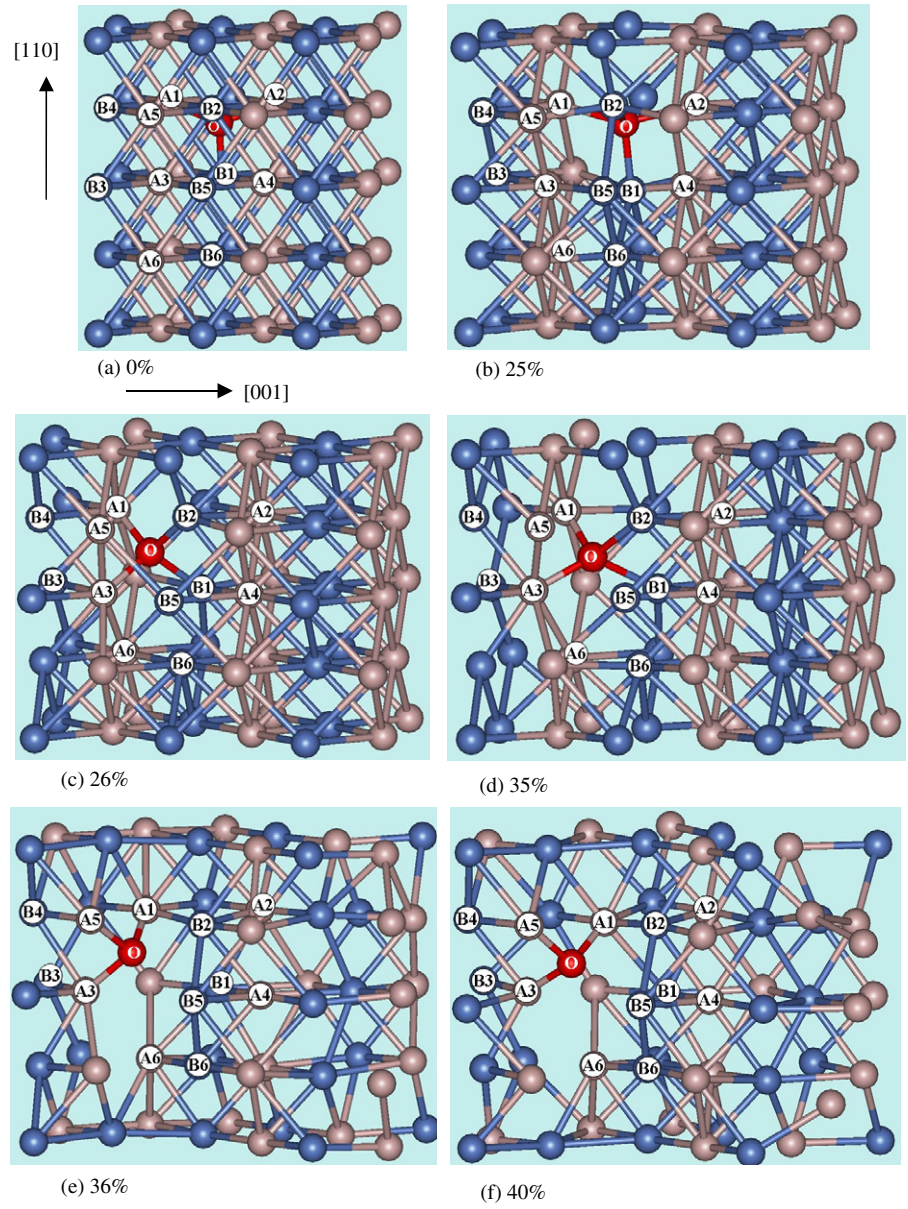

Figure 3. Evolution of the fully relaxed atomic configuration in the tensile process for NiAl with O impurity. The letters *A*, *B*, *O* represent the Al, Ni and O atoms, respectively.

strength due to the presence of O should be originated from these weaker O–Ni bonds.

3.3. Structure transformation in the tensile process

As discussed above, a structure transformation occurs at the strain of 25%. O originally (before the strain 25%) occupies one tetrahedral interstitial site surrounded by the Al atoms *A1* and *A2* and the Ni atoms *B1* and *B2* (figures 3(a) and (b)). Beyond 25%, O jumps barrierlessly to another tetrahedral interstitial site surrounded by the Al atoms *A1*and *A3* and Ni atoms *B1* and *B2* (figure 3(c)). These two configurations behaves differently in the tensile process because they have different angular configurations with respect to the [001] tensile direction. For the configuration shown in figure 5(a), the angles between two O–Al bonds and the tensile direction are 26.5° while two O–Ni bonds are normal to the tensile direction, which we call as A-type. For the configuration shown in figure 5(b), both the O–Al and O–Ni bonds form angles of 52.5° with respect to the tensile direction, which we call B-type. The strain increase causes such a structure transformation characterized by the break of one O–Al bond (*OA2*) and the formation of another O–Al bond (*OA3*).

As a matter of fact, such a structure transformation occurs incidentally since originally we happened to set the O atom in an A-type tetrahedral interstitial site as in figure 5(a). However, if O is originally set in a B-type tetrahedral interstitial site as in figure 5(b), the structure transformation cannot occur. Namely, the O–Al bond will not break, but the O–Ni bonds break instead. The stress–strain curve can be predicted to exhibit only one stress maximum instead of two. So does the energy–strain curve.

Further structure investigation show that only two types of tetrahedral interstitials exists in terms of the tensile direction.

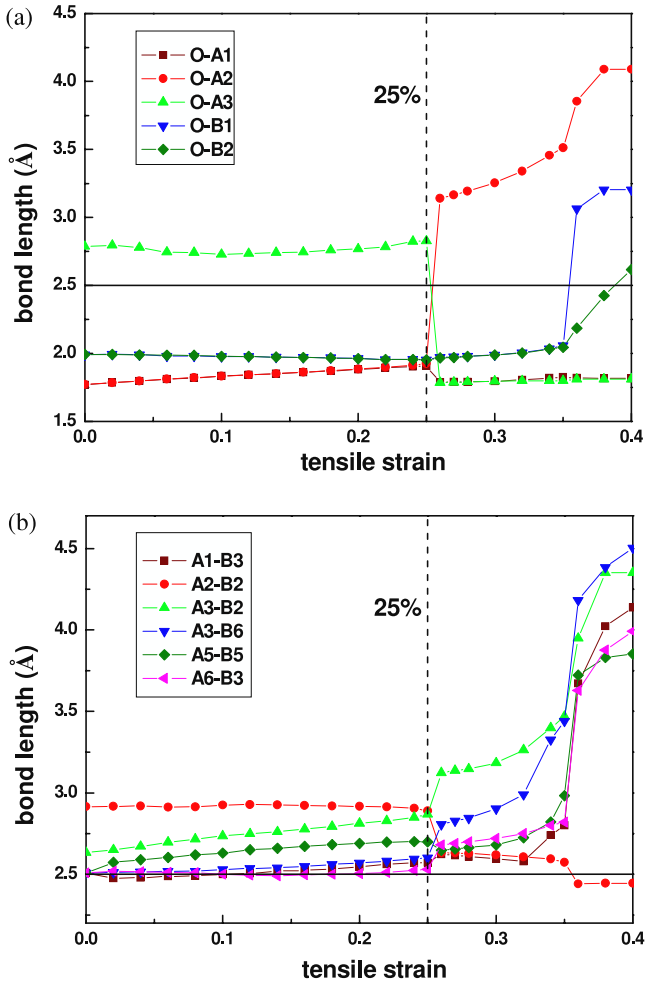

Figure 4. Atomic bonds length as a function of tensile strain. (a) Atomic bonds between O and its nearest Al and Ni atoms. (b) Atomic bonds between Ni and Al atoms. The denoted bond length of 2.5 Å by a solid line parallel to the strain axis corresponds to the length of the perfect Ni–Al bond.

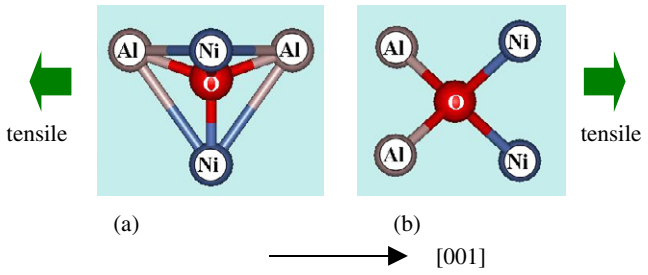

Figure 5. Two types of configurations with respect to the [001] tensile direction with O in different tetrahedral interstitial sites of NiAl.

The ratio of A-type and B-type interstitial sites is 1:2. The intrinsic of such a structure transformation is that the O–Al bonds are stronger than the O–Ni bonds. For the A-type configuration, the stress concentrates on the stronger O–Al bonds because both O–Ni bonds are normal to the tensile direction, leading to the breaking of such a stronger O–Al bond. After the O–Al fracture, the A-type structure transforms to B-type. The fracture thus occurs on the weaker O–Ni bonds because now both the O–Al and O–Ni bonds are equivalent with respect to the tensile direction. For the B-type configuration, the O–Ni bonds break directly, similar to the latter part of the A-type. Despite the different fracture modes, the tensile strength of the system should be the same as the second stress maximum (21.1 GPa) in figure 3.

Finally, we note that, without considering other instabilities such as phonon instability, the tensile strength of the present NiAl–O system should be 21.1 GPa, but the corresponding strain will not be 35% due to the existence of two different configurations in terms of the tensile direction of [001] as mentioned above. Under the tension in the ⟨001⟩ crystalline direction on the {110} plane, two types of configurations exhibit different fracture modes, but the NiAl–O system has the same tensile strength.

4. Conclusions

The ideal tensile strength and the bonding characteristics of NiAl with O impurity have been explored by performing a first-principles computational tensile test along the [001] crystalline direction on the (110) plane based on the first-principles pseudopotential scheme. We show that the tensile strength for the present supercell is reduced to 21.2 GPa due to the presence of O impurity in comparison with 37.6 GPa of pure NiAl. The atomic configuration and bond-length evolution results show that O prefers to bond with Al instead of Ni, consistent with our previous study [37]. During the tensile process, the O–Ni bonds and some Ni–Al bonds close to O–Ni break, leading to the formation of a void-like structure with the bonding of O with the Al atoms only, which can have a large effect on the mechanical properties of NiAl. We demonstrate that the fracture mode should be different with the different configurations of O in the tetrahedral interstitial sites with respect to the tensile direction, but with the same tensile strengths. The O–Ni bonds are suggested to be weaker as compared with the O–Al bonds, which is responsible for the reduced tensile strength of the NiAl with O.

Acknowledgments

The research is supported by the Aeronautics Science Foundation of China (ASFC) with grant no. 2007ZF51071 and New Century Excellent Talents in University NCET-07-0040.

References

[1] Kelly A and Macmillan N H 1986 *Strong Solids* 3rd edn (Oxford: Clarendon)
[2] Morris J W Jr, Krenn C R, Roundy D and Cohen M L 2000 *Phase Transformations and Evolution in Materials* (Warrendale, PA: TMS) p 187
[3] Morris J W Jr and Krenn C R 2000 *Phil. Mag.* A **80** 2827
[4] Hohenberg G P and Kohn W 1964 *Phys. Rev.* B **136** 864
[5] Kohn W and Sham L J 1965 *Phys. Rev.* A **140** 1133
[6] Sob M, Wang L G and Vitek V 1998 *Phil. Mag.* B **78** 653

[7] Roundy D, Krenn C R, Cohen M L and Morris J W Jr 2001 *Phil. Mag.* A **80** 1725
[8] Roundy D, Krenn C R, Cohen M L and Morris J W Jr 1999 *Phys. Rev. Lett.* **82** 2713
[9] Luo W, Roundy D, Cohen M L and Morris J W Jr 2002 *Phys. Rev.* B **66** 094110
[10] Clatterbuck D M, Krenn C R, Cohen M L and Morris J W Jr 2003 *Phys. Rev. Lett.* **91** 135501
[11] Liu Y-L, Zhang Y, Zhou H-B, Lu G-H and Kohyama M 2008 *J. Phys.: Condens. Matter* at press
[12] Liu Y-L, Zhang Y, Hong R-J and Lu G-H 2008 *Chin. Phys.* at press
[13] Li W and Wang T 1999 *Phys. Rev.* B **59** 3993
[14] Ogata S, Hirosaki N, Kocer C and Shibutani Y 2001 *Phys. Rev.* B **64** 172102
[15] Kocer C, Horosaki N and Ogata S 2003 *Phys. Rev.* B **67** 035210
[16] Li T, Morris J W Jr and Chrzan D C 2004 *Phys. Rev.* B **70** 054107
[17] Jahnátek M, Krajčí M and Hafner J 2005 *Phys. Rev.* B **71** 024101
[18] Deyirmenjian V B, Heine V, Payne M C, Milman V, Lynden-Bell R M and Finnis M W 1995 *Phys. Rev.* B **52** 15191
[19] Kohyama M 1999 *Phil. Mag. Lett.* **79** 659
[20] Kohyama M 2002 *Phys. Rev.* B **65** 184107
[21] Yamaguchi M, Shiga M and Kaburaki H 2005 *Science* **307** 393
[22] Lu G-H, Deng S, Wang T, Kohyama M and Yamamoto R 2004 *Phys. Rev.* B **69** 134106
[23] Lu G-H, Zhang Y, Deng S, Wang T, Kohyama M, Yamamoto R, Liu F, Horikawa K and Kanno M 2006 *Phys. Rev.* B **73** 224115
[24] Zhang Y, Lu G-H, Wang T, Deng S, Wang T, Kohyama M and Yamamoto R 2006 *Mater. Trans.* **47** 2678
[25] Zhang Y, Lu G-H, Hu X-L, Wang T, Kohyama M and Yamamoto R 2007 *J. Phys.: Condens. Matter* **19** 456225
[26] Zhang Y, Lu G-H, Deng S, Wang T, Xu H, Kohyama M and Yamamoto R 2007 *Phys. Rev.* B **75** 174101
[27] Stoloff N S 1996 *Microstructure and Properties of Materials* vol 1 (Singapore: World Scientific) pp 51–106
[28] Miracle D B and Darolia R 1995 *Intermetallic Compounds: Principles and Practice* vol 2 (Chichester: Wiley) pp 53–72
[29] Hong T and Freeman A J 1990 *Phys. Rev.* B **43** 6446
[30] Misra A and Gibala R 2000 *Intermetallics* **8** 1025
[31] Raynolds J E, Smith J R, Zhao G-L and Srolovitz D J 1995 *Phys. Rev.* B **53** 13883
[32] Parlinski K, Jochym P T, Schober H, Jianu A, Dutkiewicz J and Maziarz W 2004 *Phys. Rev.* B **70** 224304
[33] Jiang C, Sordelet D J and Gleeson B 2006 *Scr. Mater.* **55** 759
[34] Lazar P and Podloucky R 2006 *Phys. Rev.* B **73** 104114
[35] Djajaputra D and Cooper B R 2001 *Phys. Rev.* B **64** 085121
Djajaputra D and Cooper B R 2002 *Phys. Rev.* B **66** 205108
[36] Levit V I, Bul I A, Hu J and Kaufman M J 1996 *Scr. Mater.* **34** 1925
[37] Hu X-L, Zhang Y, Lu G-H, Wang T, Xiao P-H, Yin P-G and Xu H 2008 *Intermetallics* at press
[38] Kresse G and Hafner J 1993 *Phys. Rev.* B **47** 558
Kresse G and Furthmüller J 1996 *Phys. Rev.* B **54** 11169
[39] Vanderbilt D 1990 *Phys. Rev.* B **41** 7892
[40] Perdew J P and Wang Y 1992 *Phys. Rev.* B **45** 13244
[41] Monkhorst H J and Pack J D 1976 *Phys. Rev.* B **13** 5188
[42] Filippetti A and Fiorentini V 2000 *Phys. Rev.* B **61** 8433